Ecological Indicators 118 (2020) 106750

Contents lists available at ScienceDirect

Ecological Indicators

journal homepage: www.elsevier.com/locate/ecolind

Tree-ring lignin proxies in *Larix gmelinii* forest growing in a permafrost area of northeastern China: Temporal variation and potential for climate reconstructions

Qiangqiang Lu[a,b], Xiaohong Liu[a,c,*], Tobias Anhäuser[d,e], Frank Keppler[d,f], Yabo Wang[a], Xiaomin Zeng[a], Qiuliang Zhang[g], Lingnan Zhang[a], Keyi Wang[a], Yu Zhang[a]

[a] School of Geography and Tourism, Shaanxi Normal University, Xi'an 710119, China
[b] Key Laboratory of Soil Resource & Biotech Applications, Shaanxi Academy of Sciences, Xi'an Botanical Garden of Shaanxi Province (Institute of Botany of Shaanxi Province), Xi'an 710061, China
[c] State Key Laboratory of Cryospheric Science, Northwest Institute of Eco-Environment and Resources, Chinese Academy of Sciences, Lanzhou 730000, China
[d] Institute of Earth Sciences, Heidelberg University, Im Neuenheimer Feld 234-236, 69120 Heidelberg, Germany
[e] Department of Chemical and Physical Sciences, University of Toronto Mississauga, Mississauga L5L1C6, Canada
[f] Heidelberg Center for the Environment HCE, Heidelberg University, D-69120 Heidelberg, Germany
[g] Forest College of Inner Mongolia Agricultural University, Hohhot 010018, China

ARTICLE INFO

Keywords:
Tree rings
Lignin composition
Stable isotopes of methoxy groups
Temporal variation
Climate response

ABSTRACT

The hydrogen and carbon stable isotope ratios (δ^2H_{LM} and $\delta^{13}C_{LM}$ values) of tree-ring lignin methoxy groups have recently been recognized as valuable palaeoclimate indicators. However, the environmental factors but also sample preparation processes that might cause variations of δ^2H_{LM} and $\delta^{13}C_{LM}$ values have been not fully explored. Furthermore, the temporal dynamics of wood lignin content on both isotopes hasn't been investigated. To investigate the effects of total lignin content, removal of lipids and differences between individual and pooled tree-ring series on isotopic values, we analyzed ring samples of dominant *Larix gmelinii* trees from a typical permafrost region of northeastern China. We also examined relationships between δ^2H_{LM} and $\delta^{13}C_{LM}$ values with annual-resolution lignin content and climatic parameters over the common period of overlap 1901 to 2013. We found that the inter-tree variability between the individual and pooled isotopic chronologies was consistent, and the removal of lipids did not change the results of stable isotope measurements. The total lignin content shifted between the heartwood and sapwood, whereas the content of guaiacyl monomers (G-lignin), the only donor of methoxy groups, remained constant. Correlations analysis between lignin proxies and climate variables indicated that the heartwood total lignin content was positively correlated with the intrinsic water-use efficiency, temperature and vapor-pressure deficit (VPD), but negatively with the early-growing-season standardized precipitation evaporation index. Whilst δ^2H_{LM} values were positively correlated with the growing season temperature (May to August) and VPD, particularly in August, $\delta^{13}C_{LM}$ series showed insignificant correlation. Therefore, we suggest that the total lignin content and δ^2H_{LM} values of tree rings (both individual and pooled series) are suitable for tracking environment dynamics, as they can reveal the climate responses of tree growth.

1. Introduction

Tree-ring chronologies based on parameters such as the annual ring width, late wood density and stable isotope ratios of cellulose (δ^2H, $\delta^{18}O$ and $\delta^{13}C$ values) are widely used as climate indicators to investigate regional or global environmental change, and to establish palaeoclimate reconstructions. This is mainly because of the widespread distribution of trees and the high temporal resolution of their tree rings that can be measured for several parameters with excellent reproducibility (Esper et al., 2002; Tian et al., 2007; Gessler et al., 2010; Zeng et al., 2017; Liu et al., 2017, Liu et al., 2019a,b). However, much less research has focused on lignin attributes, even though the lignin content clearly changes during the climatic response of tree growth (Robertson et al., 2004; Coleman et al., 2008; Voelker et al., 2011; Hall et al., 2015). In the complex structure of wood, lignin is after cellulose the second most abundant biopolymer, which predominantly

* Corresponding author at: School of Geography and Tourism, Shaanxi Normal University, West Chang'an Street 620, Xi'an, Shaanxi 710119, China.
E-mail addresses: xhliu@snnu.edu.cn, liuxh@lzb.ac.cn (X. Liu).

https://doi.org/10.1016/j.ecolind.2020.106750
Received 2 April 2020; Received in revised form 28 May 2020; Accepted 19 July 2020

is formed from the oxidative radicalization of three hydroxycinnamic alcohols via β-O-4 (β-aryl ether) bonds and then deposited in the thickened secondary cell walls (Somerville et al., 2004; Vanholme et al., 2010). With its special hydrophobic traits, lignin improves the structural rigidity of xylem tissue and the transmission efficiency of source water (Pilate et al., 2012). In gymnosperms, especially in conifers, the polymerized lignin is mostly composed of monolignols, which include abundant guaiacyl units (G-lignin), with minor amounts of *p*-hydroxyphenyl units (H-lignin) and other chain-starting monomers (Armin et al., 2012; Lan et al., 2016; Vanholme et al., 2019). The types and quantities of these lignin compositions are species dependent (Bush et al., 2011), genetically determined (Nakashima et al., 2008; Bonawitz and Chapple, 2010; Xia et al., 2018) and under environmental control including elevation, temperature, precipitation and light intensity (Gindl et al., 2000; Silva Moura et al., 2010; Baxter and Stewart, 2013; Dos Santos et al., 2015). From an evolutionary perspective, lignin deposition and variation of its content are the result of the lignification of dead cells in the xylem, which connected with the aging and death of the ray parenchyma cells (Honjo et al., 2005; Song et al., 2011; Lim et al., 2016). Over time, the sapwood gradually transforms into the non-living heartwood, this transformation involved in the change of chemical and physiological mechanisms in two parts of tree rings (Millers, 2013; Piqueras et al., 2020). The higher content of lignin polymers in gymnosperms leads to thicker tracheid walls, which increase survival by providing stronger biomechanical support for long-term growth and by protecting against embolism formation under water stress during warm and dry growing seasons (Jacobsen et al., 2007; Martone et al., 2009; Stackpole et al., 2011; Pereira et al., 2017; Lima et al., 2018).

Monolignol G-lignin, with strong and abundant cross-linked bonds, is a rigid and hydrophobic substrate (Koehler and Telewski, 2006; Saito et al., 2012) that contains ether bonded methoxy (–OCH_3) groups, which formed during the methylation of *S*-adenosyl-L-methionine, and depends on caffeic acid 3-O-methyltransferase during lignin biosynthesis (Lam et al., 2007; Maury et al., 2010). These –OCH_3 groups are precursors for C1 volatiles in the environment (Keppler et al., 2004) and they are of interest for palaeoclimate studies (Keppler et al., 2007). It is important to note that after lignin biosynthesis and methylation, hydrogen and carbon atoms of the lignin methoxy (LM) groups of wood do not exchange with those from source water or organic components/metabolites. Thus, after biochemical formation the initial $^{2}H/^{1}H$ and $^{13}C/^{12}C$ ratios of wood LM groups ($\delta^{2}H_{LM}$ and $\delta^{13}C_{LM}$ values, respectively) will be unaffected during further tree growth (Keppler et al., 2004, 2007; Greule et al., 2015; Sessions, 2016). Furthermore, it has been suggested that $\delta^{2}H_{LM}$ and $\delta^{13}C_{LM}$ values of dead wood do not fractionate during biotic and abiotic degradation processes (Greule et al., 2008, 2015; Anhäuser et al., 2017a), preparation of sample material and subsequent analysis (Keppler et al., 2004, Keppler et al., 2007). The measurement of $\delta^{2}H_{LM}$ and $\delta^{13}C_{LM}$ values is usually determined by the Zeisel method (Zeisel, 1885) – the substitution reaction between the woody –OCH_3 groups and hydroiodic acid (HI) to quantitatively form gaseous methyl iodide (CH_3I). Subsequently, $\delta^{2}H_{LM}$ and $\delta^{13}C_{LM}$ values of plant methoxy groups have been widely applied into biogeochemical, atmospheric, palaeoclimatic but also forensic studies (Greule et al., 2008, 2009, Greule and Keppler, 2011, 2015, 2019, 2020; Gori et al., 2013; Mischel et al., 2015; Anhäuser et al., 2017a,b, Anhäuser et al., 2018, Anhäuser et al., 2019, 2020; Lee et al., 2019; Meier-Augenstein, 2019; Meier-Augenstein and Schimmelmann, 2019; Wang et al., 2020).

Previous studies have clearly shown that the isotopic composition of precipitation is mainly controlled by latitude, altitude and temperature (Dansgaard, 1964; Bowen and Wilkinson, 2002) but also continental effects might play a role (Hoogewerff et al., 2019). The $\delta^{2}H$ values of precipitation particularly from mid-latitude regions (40°N to 66°N) have been shown to correlate well with $\delta^{2}H$ values from plant lipids (Sternberg, 1988), bulk wood (Gori et al., 2013), tree-ring cellulose nitrate (Liu et al., 2015) and lignin methoxy groups (Keppler et al., 2007, 2008; Riechelmann et al., 2017; Anhäuser et al., 2017a,b, Anhäuser et al., 2020). These plant hydro-climatic relationships are driven by the root and xylem transport systems and their responses to temperature, leaf transpiration and VPD (Tang et al., 2000; Feakins et al., 2013; Hepp et al., 2017). Even though cellulose and LM groups share the hydrogen atoms of soil water as a common source, subsequent biochemical pathways (associated with isotope fractionation) define cellulose- derived $\delta^{2}H$ values primarily as a proxy for leaf water $\delta^{2}H$ values and LM groups for $\delta^{2}H$ values of xylem water (Feakins et al., 2013; Anhäuser et al., 2020). In particular, the strong response to temperature-induced changes in $\delta^{2}H$ values of meteoric water (Dansgaard, 1964) is well reflected in $\delta^{2}H_{LM}$ values of tree rings (Feakins et al., 2013; Anhäuser et al., 2017b). The recent work of Anhäuser et al. (2019, 2020) confirmed that $\delta^{2}H_{LM}$ values have great potential to reconstruct regional palaeotemperature from trees of mid-latitude areas, and even be applicable for reconstructing large-scale temperature changes including atmospheric circulation patterns. Other studies measuring $\delta^{13}C_{LM}$ values from alpine but also from low-altitude environments showed relationships to temperature, precipitation and vapor-pressure deficit (VPD) (Gori et al., 2013; Mischel et al., 2015; Riechelmann et al., 2016).

However, there still exist no information about the relationships between climate parameters and annual-resolution $\delta^{2}H_{LM}$ and $\delta^{13}C_{LM}$ values with respect to the total lignin and G-lignin content. Furthermore, the traditional strategies of tree-ring isotope analyses using cellulose have suggested that mass-weighted pooled samples might be appropriate for obtaining reliable isotopic chronologies (Leavitt, 2008; Liu et al., 2015). Finally, the effect of lipid removal (degreasing) from bulk wood material might also affect stable isotope values (Greule et al., 2019; Lee et al., 2019). Therefore, we attempted to fill some of the gaps in our knowledge by comparing the individual and pooled tree-ring series, the procedure of degreasing and the potential relationship of total lignin and G-lignin content with $\delta^{2}H_{LM}$ and $\delta^{13}C_{LM}$ values. All these investigated tree-ring wood from *Larix gmelinii* (larch), which is the dominant deciduous tree species in the Greater Hinggan Mountains and significantly influenced by the harsh permafrost environment.

Previous studies of tree-ring widths in northeastern China indicated that the dynamics of forest growth were highly sensitive to the warming growing season and increasing water stress (Liu et al., 2009; Zhang et al., 2014; Chen et al., 2015). Our recent studies (Liu et al., 2017, 2019a; Zhang et al., 2018), which based on permafrost forest tree-ring cellulose $\delta^{13}C$ and $\delta^{18}O$ chronologies, demonstrated that tree growth have affected by the combined effects of temperature and intrinsic water-use efficiency (iWUE). Specifically, the summer VPD and relative humidity (RH) were the dominant factors, and strongly regulated stomatal conductance, which in turn controlled iWUE.

In the present study, we investigated the temporal dynamics of several potential lignin proxies and their response to climatic parameters. We hypothesized that a higher lignin content would help trees cope with the stronger water stress created by the warming environment and would thereby improve iWUE. We also hypothesized that $\delta^{2}H_{LM}$ and $\delta^{13}C_{LM}$ values, where in the cold and humid study area, might record the shorter growing season climate signals. To test these hypotheses, our specific objectives were to: (i) assess the variability of $\delta^{2}H_{LM}$ and $\delta^{13}C_{LM}$ values among individual and in pooled tree-ring samples and whether degreasing of the bulk wood does affect stable isotope measurements; (ii) evaluate the simultaneous responses of total lignin content and climate parameters, and their correlation with iWUE; and (iii) estimate the potential of $\delta^{2}H_{LM}$ and $\delta^{13}C_{LM}$ values as climatic proxies in this high-latitude permafrost forest ecosystem.

2. Materials and methods

2.1. Sample materials

Twenty-six larch tree cross-sections at breast height were collected from Yue'AnLi forest (50°55′N, 122°21′E, 850 to 900 m a.s.l.) near

Genhe City during a forest harvesting operation in the spring of 2014 (Fig. S1). Seven tree discs with integral morphology from different trees were selected and divided each disc into eight equal sectors (Fig. S2). For each sector, tree-ring widths was analyzed using the LINTAB 6 measuring system (Rinntech, Heidelberg, Germany) with a resolution of 0.001 mm, and cross-checked the widths against previously reported data (Zhang et al., 2018) for the same tree species in a similar habitat near the present study site (sites L1, L2 and L3; Fig. S1). Results confirmed that the results were representative of trees in this region. The correlation was strong and significant (mean $r = 0.71$, $n = 113$, $P < 0.001$; Fig. S3a). Finally, four trees with unobvious growth discrepancy and with a significant inter-tree correlation were selected (Fig. S3b, Table S1) to develop raw tree-ring width (RTW) chronologies and to measure δ^2H_{LM} and $\delta^{13}C_{LM}$ values, total lignin and G-lignin content. We also considered potential juvenile effects on stable isotope measurements (Labuhn et al., 2014) by discarding the first 20 years of the samples, and the resulting time period was from 1901 to 2013.

2.1.1. Sample treatment

One sector from each of the four retained tree discs (Fig. S3b) was randomly selected, and tree rings were carefully excised with a scalpel under a dissecting microscope. The wood samples were ground to a diameter < 0.1 mm in a planetary ball mill (Pulverisette 23, Fritsch, Oberstein, Germany). To compare the variation of δ^2H_{LM} and $\delta^{13}C_{LM}$ values from the individual trees, arithmetic mean and pooled series, the tree-ring samples were divided into two subsets and treated with different strategies (for details please see below).

2.1.2. Mass-weighted series

The tree-ring samples from each tree were pooled by equal weight proportions. This mass-weighted strategy was first proposed by Treydte et al. (2001), and subsequently applied by other tree-ring studies using stable isotope analysis (Treydte et al., 2006; Leavitt et al., 2010; Szymczak et al., 2012; Liu et al., 2015).

2.1.3. Individual trees and arithmetic mean series

To retain the characteristics of individual trees, we first performed independent isotopic chronologies for each tree, and then calculated arithmetic mean values (Gagen et al., 2007; Leavitt et al., 2010; Liu et al., 2012). According to the measurement approach of three-year interval, isotope sequence was acquired from the selected sectors of each discs, counting for 38 isotope data (i.e., 1901, 1904, 1907, ···, 2006, 2009, 2012).

2.2. Analytical measurements

Before chemical treatment and analysis, all the pooled powder samples were thoroughly homogenized using vortex mixers (VORTEX-5, Kylin-Bell, Haimen, China) and subsequently oven-dried at 50 °C under vacuum in a desiccator for 48 h. Whether it is necessary to pool the tree-ring samples in the same calender year of four trees, which depends on the correlation of individual and pooled isotope series. For a more detailed description of the experimental protocol we would like to refer to Fig. S4.

2.2.1. Stable isotope analysis

To test whether removal of lipids from bulk wood (ground wood without any further preparation called 'bulk') affects δ^2H_{LM} and $\delta^{13}C_{LM}$ values, samples from the middle (1932 to 1982) of the full time period were selected. Soxhlet mixture solvent of toluene and ethanol (v/v, 32:68) was applied to remove lipids from the bulk wood under 75 °C for two hours (Loader et al., 1997), and then the solvents were volatilized to obtain the degreased wood samples.

To prepare CH_3I samples from tree-ring wood for measurements of δ^2H_{LM} and $\delta^{13}C_{LM}$, we followed the methods of Keppler et al. (2007) and Greule et al. (2008, 2009) with minor modifications (see section 1.1 of the Supplemental Material for details). All measurements were performed using gas chromatography-pyrolysis combustion-isotope ratio mass spectrometer (GC/Py-C/IRMS) (TRACE 1310; Thermo Fisher, Bremen, Germany). The gas chromatograph (GC) was fitted with a TG-5MS column (30 m × 0.25 mm × 0.25 μm; Thermo Fisher, Bremen, Germany). The stability and parallelism of GC/Py-C/IRMS were examined by repeated experiments (n = 30) of the known single tree-ring samples (mean ± SD values, −296.0 ± 5.0‰ for δ^2H_{LM} and −35.0 ± 0.3‰ for $\delta^{13}C_{LM}$). And this working standard was measured in every ten analytical samples to assess the reproducibility of the isotope measurements and normalization.

The isotope labeling CH_3I from commercial standard is liquid and highly corrosive to chromatographic columns, so both stable isotope measurements were normalized with reference gas H_2 (−214.66‰, V-SMOW) and CO_2 (−39.26‰, V-PDB) by one-point anchored method (Zeng et al., 2017). The authors are aware that this procedure represents a one-point calibration and has its limitations as it does not follow the principle of identical treatment of samples and reference materials (Werner and Brand, 2001). Thus, both the δ^2H_{LM} and $\delta^{13}C_{LM}$ values might be affected by additional errors such as "scale compression" (Meier-Augenstein and Schimmelmann, 2019). However, the measured δ^2H_{LM} and $\delta^{13}C_{LM}$ values and the observed relative differences of the wood samples were sufficient to answer the specific research questions of this paper.

Due to the anthropogenic release (mainly from fossil fuel burning) of CO_2 to the atmosphere, mixing ratios of CO_2 increased from around 280 parts per million by volume (ppmv) at CE 1800 to 410 ppmv today (Francey et al., 1999) (NOAA Mauna Loa CO_2 Data, www.co2now.org). Since the anthropogenic CO_2 has more negative $\delta^{13}C$ value than the atmosphere, the $\delta^{13}C$ value of the atmosphere decreased substantially within the last 150 years. This effect is also known as the Suess effect (Keeling, 1979) and needs to be considered when analysing, comparing and discussing tree-ring $\delta^{13}C$ values from trees grown in the period from 1850 until today. Therefore, the $\delta^{13}C_{LM}$ series were corrected to account for rising $\delta^{13}C$ values of atmospheric CO_2 using the method of McCarroll and Loader (2004). This is valid for all $\delta^{13}C$ data shown in the results and discussion section.

2.2.2. Lignin content

The acetyl bromide method developed by Johnson et al. (1961) was applied to measure the lignin content of the wood. Briefly, the analytical concept depends on the free hydroxyl (α-carbon and γ-carbon) that is characteristic of the side-chain in the phenylpropane. Acetylation and bromination occurs under acetic acid conditions to form lignin derivatives, which show special absorbance at 280 nm. The acetyl bromide lignin was prepared by using the improved method of Hatfield and Fukushima (2005). The standard alkali-lignin (TCI, Tokyo, Japan) was used for calibration. For details please refer to section 1.2 of the Supplemental Material.

2.2.3. Lignin monomer composition

Quantification of the lignin monomer composition was accomplished by thiolysis, which can effectively cleave ether linkages and yield thioester derivatives, which can then be analyzed by means of gas chromatography mass spectrometer (GC/MS) and confirmed based on data for molecular ions and the internal standard (Lapierre et al., 1986; Robinson and Mansfield, 2009). The final determination of the lignin monomer content was based on the method of Harman-Ware et al. (2016). For details please refer to Section 1.3 of the Supplemental Material.

2.3. Statistical analysis

The sampling site in the present study is the same as described in our previous studies (Liu et al., 2017, 2019a; Zhang et al., 2018). The regional climate conditions are similar, and the same larch species were

collected (Fig. S1). Therefore, the existing mean meteorological data for the common period 1957 to 2013 was used, which including the monthly temperatures, total precipitation, RH and the calculated standardized precipitation evaporation index (SPEI) and VPD. All these climatic factors and the annual iWUE from arithmetic average values of multi-sampling sites (Fig. S1; L1, L2 and L3) were participated in subsequent correlation analysis.

The correlation between annual records (RTW, δ^2H_{LM} and $\delta^{13}C_{LM}$ values, total lignin and G-lignin content and iWUE) of larch and climate parameters (monthly and seasonal factors) of previous October to the current calendar year were calculated by Pearson's coefficient (r) using SPSS 20.0 (IBM, Chicago, USA), and including high-frequency variations (first-order differences). The strength of the fitting of the linear relationships among parameters was determined using the regression goodness of fit (R^2). We quantified the differences between individual series using the standard deviations (SDs) and the Gleichläufigkeit (GLK) parameter, which represents proportion of the total number of dates when two series show the same variation trend in relation to the preceding year (Schweingruber et al., 1993). The Lag-1 autocorrelation (AR1) was used to represent the existence of a time lag in the relationships (Khaliq and Cunnane, 1996), and to describe the standard normal distribution using the skewness (SKE) and kurtosis (KUR); as SKE and KUR approach 0, the distribution of our dataset become increasingly symmetric (Suárez and Thorne, 2009).

3. Results

3.1. Comparison of individual and pooled tree-ring chronologies

The mean RTW values (Fig. 1a) of the four individual larch trees chosen for the analytical period had highly significant Pearson correlation ($r = 0.90$, $P < 0.001$) and GLK value (78.0%, $P < 0.001$), which suggested that these trees were controlled by similar regional environmental conditions, and thereby could be appropriate for the pooling samples for the lignin-related measurements. The Z-score trends for the three-year interval δ^2H_{LM} and $\delta^{13}C_{LM}$ values (Table S1) of the four trees showed a consistent pattern with moderately strong, but

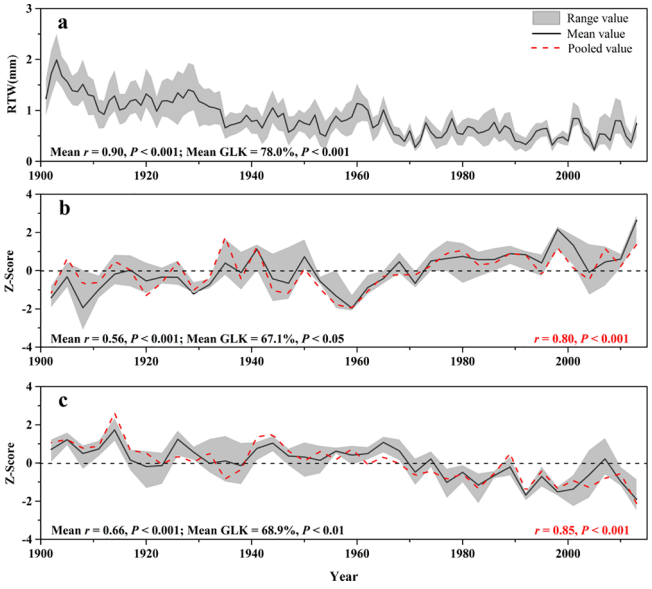

Fig. 1. (a) The raw tree-ring width (RTW) series for the four individual trees used for lignin indicators study and their annual-resolution values from 1901 to 2013. The Z-score series for (b) δ^2H_{LM} and (c) $\delta^{13}C_{LM}$ values of individual trees in the lignin methoxy groups with three years interval resolution ($n = 38$). Mean correlations (Pearson's r) and Gleichläufigkeit (GLK) values indicate the consistency among the individual trees; the red r and P values in panels (b) and (c) represent the consistency between the mean and pooled values.

significant mean correlation of δ^2H_{LM} ($r = 0.56$, $P < 0.001$; Fig. 1b) and $\delta^{13}C_{LM}$ values ($r = 0.66$, $P < 0.001$; Fig. 1c), respectively. Particularly, the correlations between the arithmetic mean and pooled methoxy isotope chronologies were very strong ($r = 0.80$ for δ^2H_{LM} and 0.85 for δ^2C_{LM}, $P < 0.001$; Fig. 1b & c), which showed convincing tree-growth synchronicity for the investigated periods. In addition, even though some GLK values between two trees were insignificant, the mean values among the four trees did significant (67.1% for δ^2H_{LM}, $P < 0.05$ and 68.9% for $\delta^{13}C_{LM}$, $P < 0.01$; Fig. 1b & c), which again demonstrate that the pooled isotopes can account for the contribution of each tree to the mean values. In the following measurements, the annual tree-ring samples were pooled with mass-weighted strategy.

3.2. δ^2H_{LM} and $\delta^{13}C_{LM}$ values from bulk wood and after removal of lipids

The trends for δ^2H_{LM} and $\delta^{13}C_{LM}$ values were relatively consistent from 1932 to 1982, with $r = 0.73$ ($P < 0.001$; Fig. S5a) and $r = 0.59$ ($P < 0.001$; Fig. S5b) for two wood samples, respectively. The range between the maximum and minimum values of each bulk wood tree-ring series were lower (41.25 and 3.71‰, respectively) than those for the degreased series (53.26 and 4.10‰, respectively), and the SDs for both parameters from the bulk wood data (9.52 and 0.90, respectively) were also less than those for the degreased data (11.16 and 0.98, respectively) (Table 1). Despite these differences, one-way ANOVA revealed insignificant difference between the δ^2H_{LM} and $\delta^{13}C_{LM}$ values of the differently treated wood series. The first-order AR1 values between the different samples were all similarly strong and significant ($P < 0.05$), with values of 0.47 and 0.51 for the δ^2H_{LM} series and 0.49 and 0.51 for $\delta^{13}C_{LM}$ series, respectively (Table 1). From the Gaussian distribution, the SKE and KUR values of the bulk wood δ^2H_{LM} series were not greatly different from 0 (−0.18 and 0.01, respectively), indicating a relatively normal distribution, whereas the corresponding values from the degreased wood were 0.45 and 0.62, suggesting a positively skewed and mesokurtic distribution (Table 1). Although the negative SKE values in both $\delta^{13}C_{LM}$ series were similar (−0.37 and −0.33, respectively), the negative KUR values of the two series were quite different (−0.24 and −0.65, respectively), indicating that the bulk wood series were closer to a normal distribution than the degreased values (Table 1).

3.3. Relationships between the tree-ring lignin content, monomer composition and isotopic chronologies

The tree discs showed a clear visual boundary between the heartwood and sapwood around 1988 (Fig. S2). The temporal variation of the tree-ring lignin content (in the range of 4.8–15.2%) showed a typical depositional pattern, with a significant increasing trend in the heartwood (slope = 0.47 per decade, $R^2 = 0.55$, $n = 88$, $P < 0.001$; Fig. 2a), followed by a rapid decrease and rapid recovery to just below the 1988 level in the transition region and sapwood. Overall, the total lignin content in the heartwood was greater than that of the sapwood (Fig. S6a). However, the G-lignin chronologies showed insignificant trend throughout the investigated time period (Fig. 2b, Fig. S6b), and no measureable amounts of H-lignin could be determined in the GC–MS analysis (Fig. S6c). Scatterplots of the relationships between the G-monomer ratio (G-lignin/total lignin) and the total lignin and G-lignin content showed weak but significant linear relationships (Fig. 3), with stronger relationships in the heartwood ($R^2 = 0.33$ and 0.58, $n = 88$, $P < 0.001$; Fig. 3b & d) than for the entire investigated time period ($R^2 = 0.31$ and 0.49, $n = 113$, $P < 0.001$; Fig. 3a & c). However, no distinct change in RTW or δ^2H_{LM} and $\delta^{13}C_{LM}$ values between the sapwood and heartwood but also insignificant correlation between the G-lignin content and δ^2H_{LM} and $\delta^{13}C_{LM}$ values of the wood sample could be observed (data not shown).

Table 1
Statistical characteristics of the δ^2H_{LM} and $\delta^{13}C_{LM}$ series for the bulk and degreased wood samples for the analytical period from 1932 to 1982. Abbreviations: Max., maximum values; Min., minimum values; SD, standard deviation; Range, the difference between the maximum and minimum values; AR1, Lag-1 autocorrelation; SKE, skewness; KUR, kurtosis.

	Form	Max.	Min.	Mean	SD	Range	AR1	SKE	KUR
δ^2H_{LM} (‰)	Bulk	−288.80	−330.05	−308.79	9.52	41.25	0.47*	−0.18	0.01
	Degreased	−281.47	−334.73	−311.95	11.16	53.26	0.51*	0.45	0.62
$\delta^{13}C_{LM}$ (‰)	Bulk	−33.91	−37.62	−35.28	0.90	3.71	0.49*	−0.37	−0.24
	Degreased	−33.21	−37.31	−35.07	0.98	4.10	0.51*	−0.33	−0.65

Significance: * $P < 0.05$.

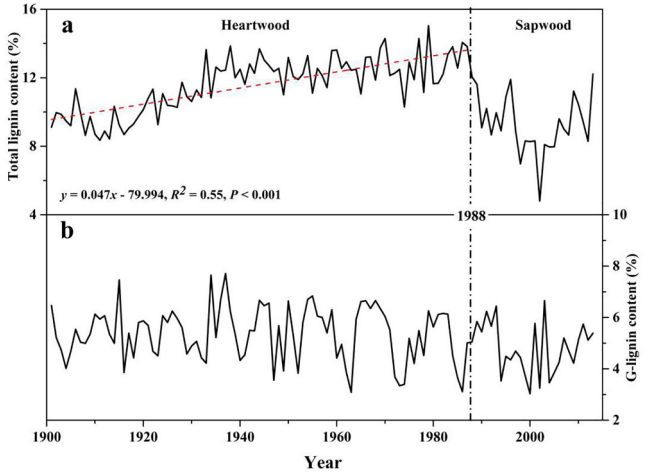

Fig. 2. The temporal variation of the tree-ring lignin content for (a) total lignin and (b) G-lignin from 1901 to 2013. The red dashed line represents the linear fitting of the total lignin content in the heartwood.

3.4. Linkages between the lignin content of the heartwood, iWUE and the climatic variables

There was a similar variation trend between total lignin content and iWUE before 1988 in the heartwood (for lignin, slope = 0.047, $R^2 = 0.55$, $P < 0.001$; for iWUE, slope = 0.142, $R^2 = 0.49$, $P < 0.001$; Fig. 4a), and the two variables were also weakly but significantly positively related ($R^2 = 0.23$, $P < 0.001$; Fig. 4b), as well as in the high-frequency variations ($r = 0.31$, $P < 0.005$; Fig. 4c). Furthermore, although the correlation in the heartwood between the total lignin content and monthly climatic factors from 1957 to 1988 was generally weak, some statistically significant correlations were found for the early growing season (Fig. 5). The total lignin content was positively correlated with the mean and maximum temperatures and VPD, but negatively correlated with SPEI in May (Fig. 5a), and these month-scale correlations remained significant based on the high-frequency variations (Fig. 5b).

3.5. Lignin methoxy isotope trends and climatic responses

During the time period of 1957 to 2013, the δ^2H_{LM} chronologies were significantly correlated with different climate parameters (Fig. 6).

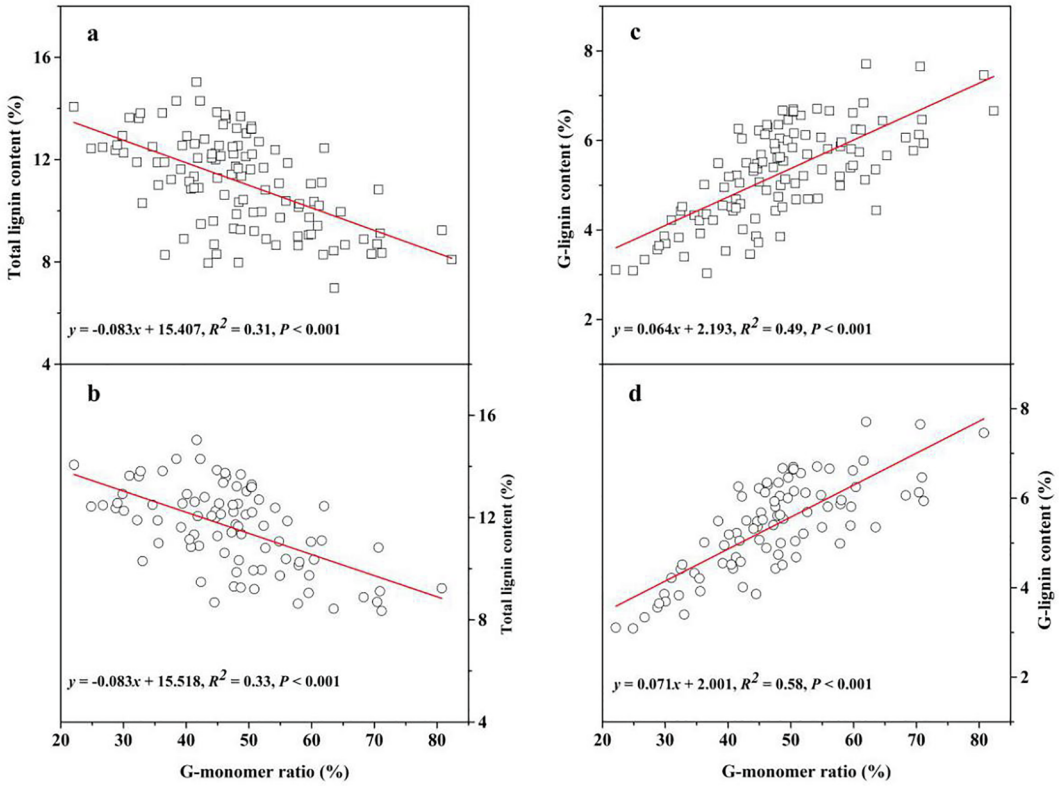

Fig. 3. Scatterplots of the relationships between (a, b) the total lignin content and (c, d) the G-lignin content and the G-monomer ratio (G-lignin/total lignin). Analyses are for (a, c) the whole measurements time and (b, d) the heartwood period. Red solid lines indicate the linear fitting of the trend.

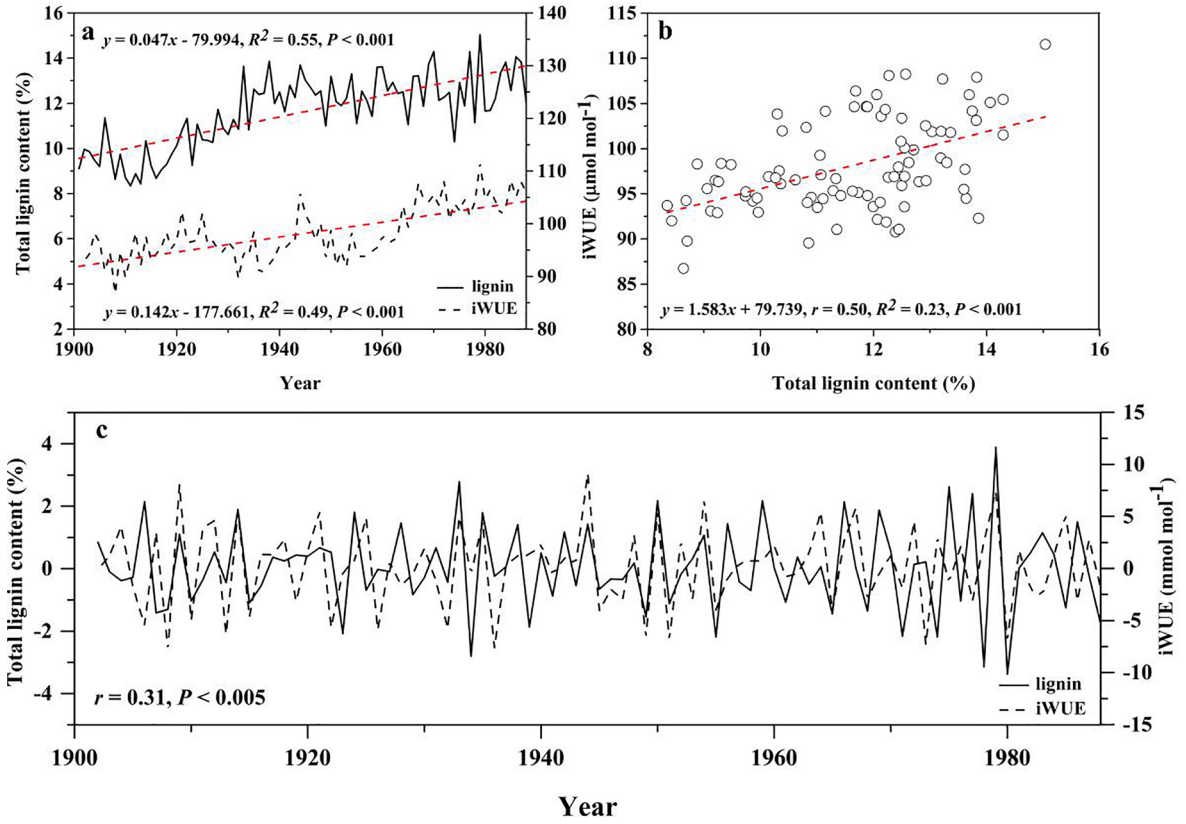

Fig. 4. (a) Comparison of temporal trends in the total lignin content and intrinsic water-use efficiency (iWUE) in the heartwood. (b) Relationship between iWUE and the total lignin content in the heartwood. (c) High-frequency variations (first-order differences). Red dashed lines indicate the linear fitting function.

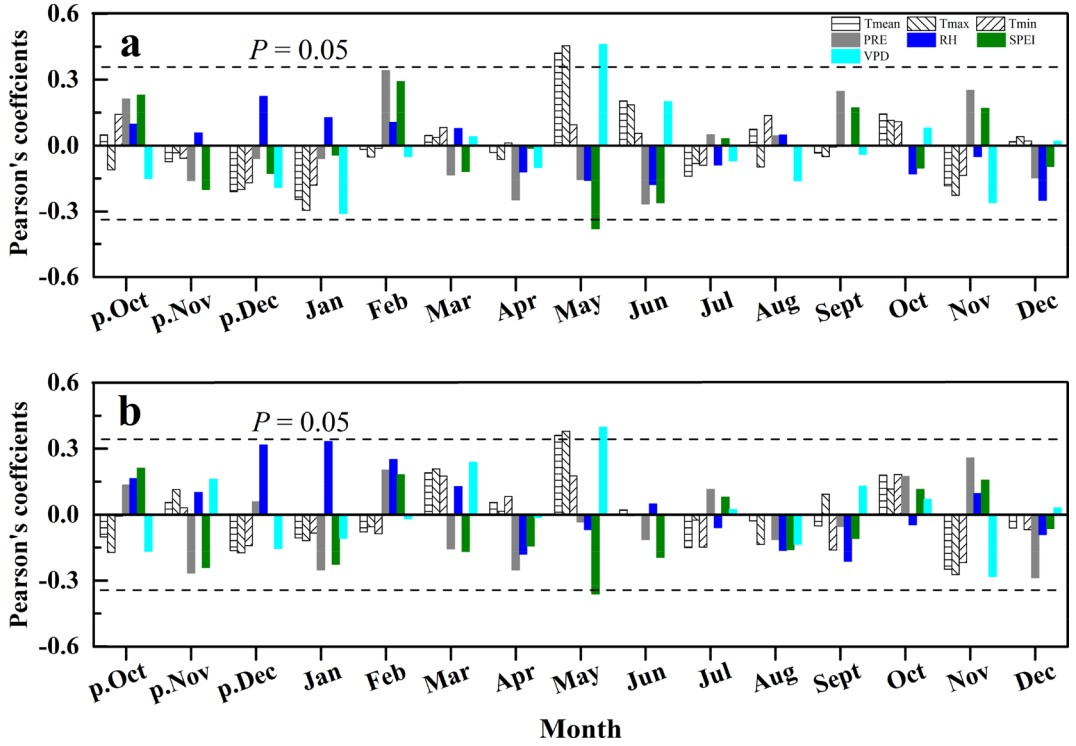

Fig. 5. Pearson's coefficients (r) for the correlation between the total lignin content and the climatic parameters in the heartwood from 1957 to 1988. (a) Monthly data; (b) High-frequency variations (first-order differences). Months labeled with "p" represent the previous year (before formation of the growth ring). Climate parameters are: T_{mean}, mean monthly temperature; T_{max}, maximum monthly temperature; T_{min}, minimum monthly temperature; PRE, total precipitation; RH, relative humidity; SPEI, standardized precipitation evapotranspiration index; and VPD (vapor-pressure deficit). The black dashed lines represent the 95% confidence interval.

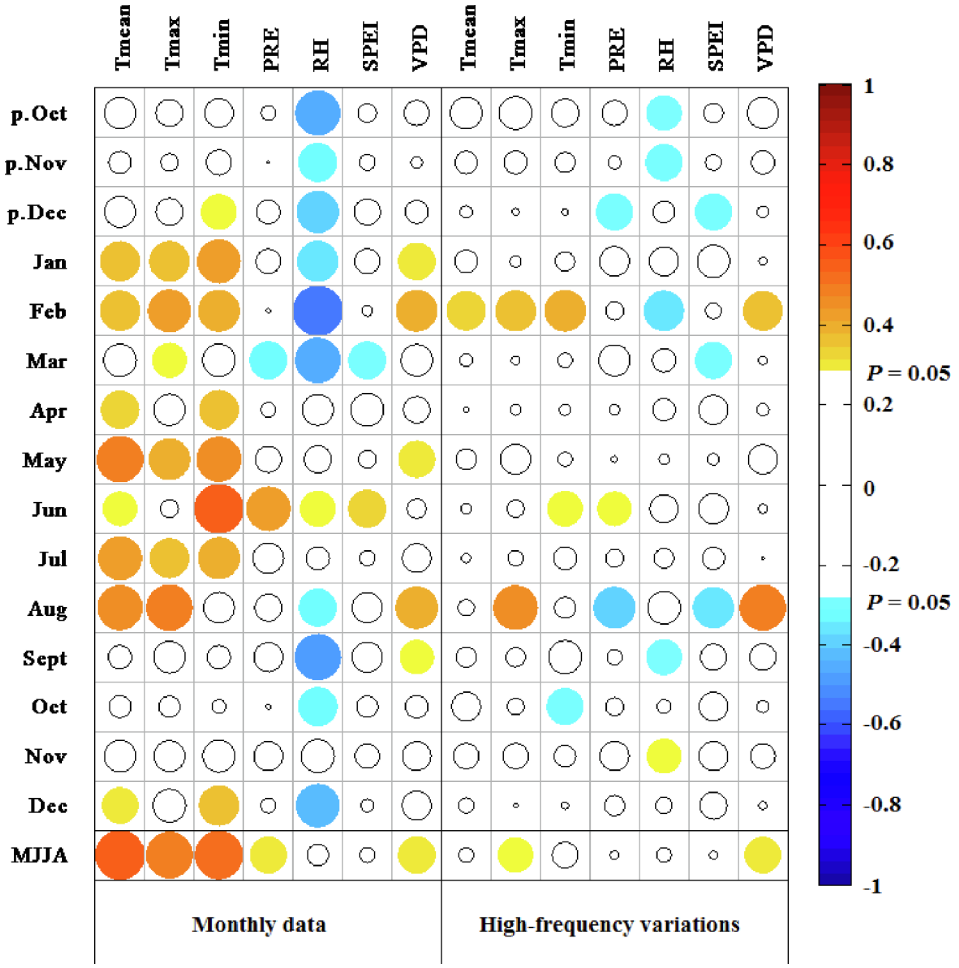

Fig. 6. Climatic responses (Pearson's *r*) of the lignin methoxy groups δ^2H_{LM} value at monthly and growing-season scales during the common period from 1957 to 2013. MJJA represents the growing season from May to August. Month names labeled with a "p" represent values in the previous year (the year before tree ring formation). The left columns are for the monthly data; the right columns are for high-frequency variations (first-order differences). The significant correlations are shown in red (positive correlations) and blue (negative correlations); the strength of the correlation is proportion to the circle's size. The white area labeled $P = 0.05$ represents the 95% confidence interval.

The strongest positive correlations were found with the temperature indices (mean, maximum and minimum), precipitation and VPD in the growing season (particularly from May to August, expressed as MJJA) (Fig. 6a), and the high-frequency variations were significantly positively correlated with maximum temperature and VPD in February and August (Fig. 6b). Specifically, the minimum temperature ($r = 0.55$, $P < 0.001$) and precipitation ($r = 0.44$, $P < 0.01$) in June and the maximum temperature ($r = 0.47$, $P < 0.001$) and VPD ($r = 0.40$, $P < 0.01$) in August were significantly positively correlated with δ^2H_{LM} values, and even in the high-frequency variations (Table S2). The δ^2H_{LM} series were also positively correlated with the three temperature parameters and VPD in January and February (Fig. 6a). Whereas, these month-scale response relations in the high-frequency variations were still significant, especially in the maximum temperature and VPD, and lasted throughout the growing season (Fig. 6b). In terms of negative correlations, these series were significantly correlated with RH outside the growing season and SPEI in March.

Interestingly, the corrected $\delta^{13}C_{LM}$ series after removing the influence of rising $\delta^{13}C$ values of atmospheric CO_2 (see Section 2.3.1) showed insignificant correlations with all the investigated climatic factors (data not shown).

4. Discussion

4.1. Inter-tree variability and effect of pooling the samples

The coherences of RTW were similar for the individual trees (Table S1) and thus suggested that the selected trees were growing in a consistent habitat and could therefore be included in the same analysis. However, the coherence of δ^2H_{LM} and $\delta^{13}C_{LM}$ values for individual trees was somewhat weaker when compared with RTW (Fig. 1, Table S1). Compared with the clear mechanistic model for isotope fractionation in tree-ring cellulose (Roden et al., 2000), those isotopic effect for lignin methoxy groups might be more complex because of the multiple regulation in lignin biosynthesis, including lignin composition and methylation. The observed difference between RTW and δ^2H_{LM} and $\delta^{13}C_{LM}$ values could be also related to analytical issues regarding measurements of stable isotope values, i.e. resulting from the combined effect of analytical uncertainties related to the reaction of $-OCH_3$ groups with HI (Greule et al., 2008, 2009), the application of reliable reference materials for δ^2H_{LM} and $\delta^{13}C_{LM}$ measurements (Greule et al., 2019, 2020), the constancy of the known stoichiometry (Lee et al., 2019) and the particle diameters of the homogenized wood powder (McCarroll and Loader, 2004).

Nevertheless, the correlations of δ^2H_{LM} and $\delta^{13}C_{LM}$ series between the mean and pooled values were highly significant ($P < 0.001$; Table S1). The arithmetic means of the four trees had a smoothing effect on the differences between individuals (Leavitt, 2008). Previous studies have shown that δ^2H_{LM} values of individual trees from the same species collected from one location can vary by up to 28‰ (Anhäuser et al., 2017a, Anhäuser et al., 2020). One explanation for the relatively large variations might be the heterogeneous source water in the soil and xylem water of the trees mainly resulting from site-specific variations in hydrology (Leavitt, 2010; Feakins et al., 2013; Anhäuser et al., 2017a). Unlike other forest districts, the hydrological condition could be even more complex in our study area because of the interplay between atmospheric rainfall, groundwater and freezing-thawing water.

4.2. Effect of removal of lipids from bulk wood

The results of δ^2H_{LM} and $\delta^{13}C_{LM}$ values for sections of the heartwood showed that the removal of lipids from bulk wood did not significantly change δ^2H_{LM} and $\delta^{13}C_{LM}$ values when compared with those of untreated bulk wood (Fig. S5, Table 1). A likely explanation is that the wood extractives were present at low quantities and did not contain a measureable content of methoxy groups. However, these results are fully in line with previous investigations of δ^2H_{LM} and $\delta^{13}C_{LM}$ measurements from wood samples (Greule, et al., 2008, 2009, Greule and Keppler, 2011) where it has been suggested that the bulk of the methoxy content (> 95%) is related to the lignin fraction of wood. Only plant material with little lignin content such as vegetables (e.g. potatoes) might produce CH_3I at measureable quantities from other plant components than $–OCH_3$ groups that need to be considered for stable isotope measurements of plant methoxy groups (Greule and Keppler, 2011). Thus, our comparison of bulk and degreased wood again supports the previous contention that bulk wood can be directly used for preparation of CH_3I and no further treatment or extraction steps of wood are required.

4.3. Variation in the response of lignin content to climatic variables

Our findings imply that the total lignin content of bulk wood might be lower than those usually found for woody plants (around 15–36%) (Zobel and van Buijtenen, 1989; Campbell and Sederoff, 1996). This is difficult to explain but might be the special chemical nature of lignin, those polymers in plant are difficult to be separated and purified, and no appropriate “standard lignin” can be adapted to calibrate the instrument. Although there is only a small portion of total lignin may be soluble in the dilute acid solution (Hatfield and Fukushima, 2005), the applied method mainly measured the alkaline-lignin content rather than total lignin content. We further found that the arithmetic mean values of the total lignin content in the heartwood were higher than those in the sapwood, and decreased sharply in the transition area between the two types of wood, within a distance of two or three growth rings (Fig. 2a & S6a). In contrast, the G-lignin content showed insignificant change over time (Fig. 2b & S6b) and its G-monomer ratio had more significant correlation with total lignin and G-lignin content in the heartwood, respectively (Fig. 3b & d). Furthermore, the corresponding δ^2H_{LM} and $\delta^{13}C_{LM}$ values showed unobvious change around the boundary between the heartwood and sapwood, but also insignificant correlations between two content variations and methoxy isotopic values were observed. These observations may be explained by changes of the lignin content and composition in various cell types, including vascular elements, phloem fibers and vascular parenchyma, and were determined by the control of lignification (Chen and Dixon, 2007). In conifers, the transformation from sapwood to heartwood is accompanied by decreasing moisture content, death of ray parenchyma cells, disappearance of stored starch, a continuous loss of catalytic enzyme activity, termination of lignification of cell walls and accumulation of extractives in the wood (Nakada and Fukatsu, 2012). These physiological changes might explain why the tree-ring lignin content in the heartwood shows a consistent and predictable response to tree growth and environmental change.

In the present study, it was found that the lignin content of larch was mainly affected by temperature and the transpiration induced in the early growing season when the tree rings formed (Fig. 5). One possible explanation could be that warming during leaf germination stage leads much more snowmelt and permafrost thawing to undertake root-leaf water transport, more active photosynthetic assimilation will facilitate plant cell wall biosynthesis, and further deposit lignin (Crivellaro and Büntgen, 2020). In general, thickening cell walls is a crucial strategy for avoiding the development of xylem embolisms, which were driven by water stress due to drought and global warming (Pereira et al., 2017; Lima et al., 2018). Our recent study (Liu et al., 2019a) showed that iWUE increased significantly with increasing atmospheric CO_2 concentration in the study area, and increased with increasing summer temperatures and VPD, but was negatively correlated with precipitation, indicating a sensitivity to moisture conditions in this permafrost region. In the heartwood, we found a strong positive correlation between the total lignin content and iWUE (Fig. 4). Based on these findings, we hypothesize that a positive response to increasing lignin content could reinforce the thickness of cell walls, facilitate water transport and resist water stress to provide an adaptation to warming and drought by activating lignin biosynthesis.

4.4. Climate signals recorded in the methoxy groups isotope time series

Although we have observed a significant correlation between δ^2H_{LM} values and temperature during the current winter (January and February) and the growing season (MJJA) (Fig. 6), the high-frequency variations showed a weak seasonal characteristic. This may be attributed to the warming non-growing season, when air temperatures increase in February, snow cover will become shallower due to melting and the depth to frozen soil will decrease. The resulting increased soil water promotes the formation of a warmer and more humid habitat in the early growing season, and this phenomenon has been confirmed by the analysis of historical climate data (Zhang et al., 2014). In addition, this complex hydrothermal condition during intense transpiration stage (August) is more conducive to the absorption and transmission of source water by trees (Ferrer et al., 2008; Ishida et al., 2008; Groenendijk et al., 2016; Crivellaro and Büntgen, 2020). Furthermore, in agreement with results from Mischel et al. (2015), we clearly found that δ^2H values strongly reflect annual maximum temperatures, but also show correlations with minimum and mean temperatures (Fig. 6).

In the uncorrected $\delta^{13}C_{LM}$ series, we found a significant positive correlation with RTW ($r = 0.63$, $n = 113$, $P < 0.001$; figure not shown), which confirms the results of previous research (Kagawa et al., 2003; Tardif et al., 2008), in which the positive correlations between $\delta^{13}C$ values of cellulose and tree-ring width usually indicated a moist environment. However, we did not find significant correlations between the corrected $\delta^{13}C_{LM}$ series and climate parameters, which indicate that measurements of $\delta^{13}C_{LM}$ values may have their limitations to be used as climate proxies in certain environments. A possible explanation is that cellulose is formed from leaf sugars produced by photosynthetic pathways for carbon fixation (Farquhar et al., 1982; Farquhar and Lloyd, 1993; Treydte et al., 2001; Verheyden et al., 2005; Cullen et al., 2008; Knorre et al., 2010; Zeng et al., 2017), whereas the methylation of lignin monomers involves a different series of complex biochemical processes (Li et al., 1997; Zabala et al., 2006; Hisano et al., 2009; Baxter and Stewart, 2013).

5. Conclusions

Our findings show that both the mean of individual and the pooled isotope series of larch similarly correlate with most of the climate parameters. The great benefit of the pooling method for application of δ^2H_{LM} and $\delta^{13}C_{LM}$ values is the considerable reduction in measurement and preparation time, whilst containing more high-frequency signals, which integrated the single-tree chronologies and provided sufficient information on climatic and ecological elements. Moreover, our results suggest that removal of lipids from bulk wood is not necessary for the determination of δ^2H_{LM} and $\delta^{13}C_{LM}$ values.

Lignin deposition in the heartwood increased over time, and the total lignin content was greater than that in the sapwood. In contrast, G-lignin remained relatively constant around the transition wood, and no shift occurred in δ^2H_{LM} and $\delta^{13}C_{LM}$ series. The heartwood total lignin content was positively correlated with iWUE, maximum temperature and VPD, but negatively with SPEI at the early growing season. This supports our hypothesis that a higher lignin content might help trees to cope with the stronger water stress created by the global warming by

improving iWUE. Consistent with previous studies, the δ^2H_{LM} chronologies were most sensitive to climate parameters, especially for growing season temperature and VPD in this permafrost region, and further indicating its potential in palaeotemperature and plant ecophysiological investigation.

6. Credit author statement

We declare that all the data and materials provided in this paper are true and valid. All the authors abide by the professional ethics and follow the scientific truth. No dishonest behavior and economic interests were occurred.

Declaration of Competing Interest

The authors declare that they have no known competing financial interests or personal relationships that could have appeared to influence the work reported in this paper.

Acknowledgments

We are grateful for the financial support provided by the Fundamental Research Funds for the Central Universities (Project No. 2019TS017, GK201801007, 2020CBLY010 & 202007012). This research was partially supported by the National Natural Science Foundation of China (Grant No. 41971104), the Open Foundation of the State Key Laboratory of Loess and Quaternary Geology, Institute of Earth Environment, Chinese Academy of Sciences (Grant No. CASSKLLQG1817), and the Science and Technology Program of Shaanxi Academy of Sciences (Grant No. 2018 k-11). We thank the Biogeochemistry group of Heidelberg University for advice regarding measurement of lignin methoxy groups stable isotopes. We also greatly appreciated suggestions from anonymous reviewers and editor staff for the improvement of our manuscript.

Appendix A. Supplementary data

Supplementary data to this article can be found online at https://doi.org/10.1016/j.ecolind.2020.106750.

References

Anhäuser, T., Greule, M., Keppler, F., 2017a. Stable hydrogen isotope values of lignin methoxyl groups of four tree species across Germany and their implication for temperature reconstruction. Sci. Total Environ. 579, 263–271. https://doi.org/10.1016/j.scitotenv.2016.11.109.

Anhäuser, T., Greule, M., Polag, D., Bowen, G.J., Keppler, F., 2017b. Mean annual temperatures of mid-latitude regions derived from δ^2H values of wood lignin methoxyl groups and its implications for paleoclimate studies. Sci. Total Environ. 574, 1276–1282. https://doi.org/10.1016/j.scitotenv.2016.07.189.

Anhäuser, T., Hook, B.A., Halfar, J., Greule, M., Keppler, F., 2018. Earliest Eocene cold period and polar amplification-insights from δ^2H values of lignin methoxyl groups of mummified wood. Palaeogeogr. Palaeocl. Palaeoecol. 505, 326–336. https://doi.org/10.1016/j.palaeo.2018.05.049.

Anhäuser, T., Sehls, B., Thomas, W., Hartl, C., Greule, M., Scholz, D., Esper, J., Keppler, F., 2019. Annually resolved δ2H tree-ring chronology of the lignin methoxyl groups from Germany reflects averaged Western European surface air temperature changes. Past Clim. https://doi.org/10.5194/cp-2019-8.

Anhäuser, T., Sehls, B., Thomas, W., Hartl, C., Greule, M., Scholz, D., Esper, J., Keppler, F., 2020. Tree-ring δ^2H values from lignin methoxyl groups indicate sensitivity to European-scale temperature changes. Palaeogeogr. Palaeocl. Palaeoecol. 546, 109665. https://doi.org/10.1016/j.palaeo.2020.109665.

Armin, W., Lloyd, D., John, R., 2012. Lignification and lignin manipulations in conifers. Adv. Bot. Res. 61, 37–76. https://doi.org/10.1016/B978-0-12-416023-1.00002-1.

Baxter, H., Stewart Jr, C., 2013. Effects of altered lignin biosynthesis on phenylpropanoid metabolism and plant stress. Biofuels 4, 635–650. https://doi.org/10.4155/bfs.13.56.

Bonawitz, N., Chapple, C., 2010. The genetics of lignin biosynthesis: Connecting genotype to phenotype. Annu. Rev. Genet. 44, 337–363. https://doi.org/10.1146/annurev-genet-102209-163508.

Bowen, G.J., Wilkinson, B., 2002. Spatial distribution of delta O-18 in meteoric precipitation. Geology 30, 315–318. https://doi.org/10.1130/0091-7613(2002)030<0315:SDOOIM>2.0.CO;2.

Bush, D., McCarthy, K., Meder, R., 2011. Genetic variation of natural durability traits in Eucalyptus cladocalyx (sugar gum). Ann. For. Sci. 68, 1057–1066. https://doi.org/10.1007/s13595-011-0121-z.

Campbell, M.M., Sederoff, R.R., 1996. Variation in lignin content and composition. Plant Physiol. 110, 3–13. https://doi.org/10.1104/pp.110.1.3.

Chen, F., Dixon, R.A., 2007. Lignin modification improves fermentable sugar yields for biofuel production. Nature Biotechnol. 25, 759–761. https://doi.org/10.1038/nbt1316.

Chen, Z.J., Zhang, X.L., He, X.Y., Davi, N.K., Li, L.L., Bai, X.P., 2015. Response of radial growth to warming and CO_2 enrichment in southern northeast China: a case of *Pinus tabulaeformis*. Clim. Change 130, 559–571. https://doi.org/10.1007/s10584-015-1356-8.

Coleman, H.D., Samuels, A.L., Guy, R.D., Mansfield, S.D., 2008. Perturbed lignification impacts tree growth in hybrid poplar – A function of sink strength, vascular integrity and photosynthetic assimilation. Plant Physiol. 148, 1229–1237. https://doi.org/10.1104/pp.108.125500.

Cullen, L.E., Adams, M.A., Anderson, M.J., Grierson, P.F., 2008. Analyses of $\delta^{13}C$ and $\delta^{18}O$ in tree rings of *Callitris columellaris* provide evidence of a change in stomatal control of photosynthesis in response to regional changes in climate. Tree Physiol. 28, 1525–1533. https://doi.org/10.1093/treephys/28.10.1525.

Crivellaro, A., Büntgen, U., 2020. New evidence of thermally constrained plant cell wall lignification. Trends Plant Sci. https://doi.org/10.1016/j.tplants.2020.01.011.

Dansgaard, W., 1964. Stable isotopes in precipitation. Tellus 16, 436–468. https://doi.org/10.3402/tellusa.v16i4.8993.

Dos Santos, A.B., Bottcher, A., Vicentini, R., Mayer, L.S.J., Kiyota, E., Landell, M.A.G., Creste, S., Mazzafera, P., 2015. Lignin biosynthesis in sugarcane is affected by low temperature. Environ. Exp. Bot. 120, 31–42. https://doi.org/10.1016/j.envexpbot.2015.08.001.

Esper, J., Cook, E.R., Schweingruber, F.H., 2002. Low-frequency signals in long tree-ring chronologies for reconstructing past temperature variability. Science 295, 2250–2253. https://doi.org/10.1126/science.1066208.

Farquhar, G.D., O'Leary, M.H., Berry, J.A., 1982. On the relationship between carbon isotope discrimination and intercellular carbon dioxide concentration in leaves. Austral. J. Plant Physiol. 9, 121–137. https://doi.org/10.1071/PP9820121.

Farquhar, G.D., Lloyd, J., 1993. Carbon and oxygen isotope effects in the exchange of carbon dioxide between terrestrial plants and the atmosphere. In: Ehleringer, J., Hall, A., Farquhar, G. (Eds.), Stable Isotopes and Plant Carbon-Water Relations. Academic Press, New York, pp. 47–70.

Feakins, S.J., Ellsworth, P.V., da Sternberg, L.S.L., 2013. Lignin methoxyl hydrogen isotope ratios in a coastal ecosystem. Geochim. Cosmochim. Acta 121, 54–66. https://doi.org/10.1016/j.gca.2013.07.012.

Ferrer, J.L., Austin, M.B., Stewart Jr., C.S., Noel, J.P., 2008. Structure and function of enzymes involved in the biosynthesis of phenylpropanoids. Plant Physiol. Biochem. 46, 356–370. https://doi.org/10.1016/j.gca.2013.07.012.

Francey, R.J., Allison, C.E., Etheridge, D., Trudinger, C.M., Enting, I.G., Leuenberger, M., Langenfelds, R.L., Michel, E., Steele, L.P., 1999. A 1000-year high precision record of $\delta^{13}C$ in atmospheric CO_2. Tellus 51, 170–193. https://doi.org/10.3402/tellusb.v51i2.16269.

Gagen, M., McCarroll, D., Loader, N.J., Robertson, I., Jalkanen, R., Anchukaitis, K.J., 2007. Exorcising the 'segment length curse': Summer temperature reconstruction since AD 1640 using non-detrended stable carbon isotope ratios from pine trees in northern Finland. Holocene 17, 435–446. https://doi.org/10.1177/0959683607077012.

Gessler, A., Brandes, E., Buchmann, N., Helle, G., Rennenberg, H., Barnard, R., 2010. Tracing carbon and oxygen isotope signals from newly assimilated sugars in the leaves to the tree-ring archive. Plant Cell Environ. 32, 780–795. https://doi.org/10.1111/j.1365-3040.2009.01957.x.

Gindl, W., Grabner, M., Wimmer, R., 2000. The influence of temperature on latewood lignin content in tree line Norway spruce compared with maximum density and ring width. Trees 14, 409–414. https://doi.org/10.1007/s004680000057.

Gori, Y., Wehrens, R., Greule, M., Keppler, F., Ziller, L., La Porta, N., Camin, F., 2013. Carbon, hydrogen and oxygen stable isotope ratios of whole wood, cellulose and lignin methoxyl groups of *Picea abies* as climate proxies. Rapid Commun. Mass Spec. 27, 265–275. https://doi.org/10.1002/rcm.6446.

Greule, M., Mosandl, A., Hamilton, John T.G., Keppler, F., 2008. A rapid and precise method for determination of D/H ratios of plant methoxyl groups. Rapid Commun. Mass Spec. 22, 3983–3988. https://doi.org/10.1002/rcm.3817.

Greule, M., Mosandl, A., Hamilton, John T.G., Keppler, F., 2009. A simple rapid method to precisely determine $^{13}C/^{12}C$ ratios of plant methoxyl groups. Rapid Commun. Mass Spec. 23, 1710–1714. https://doi.org/10.1002/rcm.4057.

Greule, M., Keppler, F., 2011. Stable isotope determination of ester and ether methyl moieties in plant methoxyl groups. Isot. Environ. Health Stud. 47, 470–482. https://doi.org/10.1080/10256016.2011.616270.

Greule, M., Rossmann, A., Schmidt, H.-L., Mosandl, A., Keppler, F., 2015. A stable isotope approach to assessing water loss in fruits and vegetables during storage. J. Agr. Food Chem. 63, 1974–1981. https://doi.org/10.1021/jf505192p.

Greule, M., Moossen, H., Geilmann, H., Brand, W.A., Keppler, F., 2019. Methyl sulfates as methoxy isotopic reference materials for $\delta^{13}C$ and δ^2H measurements. Rapid Commun. Mass Spec. 33, 343–350. https://doi.org/10.1002/rcm.8355.

Greule, M., Moossen, H., Lloyd, M.K., Geilmann, H., Brand, W.A., Eiler, J.M., Qi, H.P., Keppler, F., 2020. Three wood isotopic reference materials for δ^2H and $\delta^{13}C$ measurements of plant methoxy groups. Chem. Geol. 533, 119428. https://doi.org/10.1016/j.chemgeo.2019.119428.

Groenendijk, M., Cox, P.M., Booth, B.B.B., Dekker, S.C., Huntingford, C., 2016. Spatial and temporal variations in plant water-use efficiency inferred from tree-ring, eddy

covariance and atmospheric observations. Earth Syst. Dynam. 7, 525–533. https://doi.org/10.5194/esd-7-525-2016.
Hall, S.H., Silver, W.L., Timokhin, V.T., Hammel, K.E., 2015. Lignin decomposition is sustained under fluctuating redox conditions in humid tropical forest soils. Glob. Change Biol. 21, 2818–2828. https://doi.org/10.1111/gcb.12908.
Harman-Ware, A.E., Foster, C., Happs, R.M., Doeppke, C., Meunier, K., Gehan, J., Yue, F.X., Lu, F.C., Davis, M.F., 2016. Quantitative analysis of lignin monomers by a thioacidolysis method tailored for higher-throughput analysis. J. Biotechnol. 11, 1268–1273. https://doi.org/10.1002/biot.201600266.
Hatfield, R., Fukushima, R.S., 2005. Can lignin be accurately measured? Crop Sci. 45, 832–839. https://doi.org/10.2135/cropsci2004.0238.
Hepp, J., Zech, R., Rozanski, K., Tuthorn, M., Glaser, B., Greule, M., Keppler, F., Huang, Y., Zech, W., Zech, M., 2017. Late Quaternary relative humidity changes from Mt. Kilimanjaro, based on a coupled ^{2}H–^{18}O biomarker paleohygrometer approach. Quatern. Int. 438, 116–130. https://doi.org/10.1016/j.quaint.2017.03.059.
Hisano, H., Nandakumar, R., Wang, Z.Y., 2009. Genetic modification of lignin biosynthesis for improved biofuel production. Vitro Cell. Devel. Biol. Plant 45, 306–313. https://doi.org/10.1007/s11627-009-9219-5.
Honjo, K., Furukawa, I., Sahri, M., 2005. Radial variation of fiber length increment in *Acacia mangium*. IAWA J. 26, 339–352. https://doi.org/10.1163/22941932-90000119.
Hoogewerff, J., Kemp, H.F., Leng, M.J., Meier-Augenstein, W., 2019. Spatial variability of ^{2}H and ^{18}O composition of meteoric freshwater lakes in Scotland. Isot. Environ. Health Stud. 55, 237–253. https://doi.org/10.1080/10256016.2019.1609958.
Ishida, A., Nakano, T., Sekikawa, S., Maruta, E., Masuzawa, T., 2008. Diurnal changes in needle gas exchange in alpine *Pinus pumila*, during snow-melting and summer seasons. Ecol. Res. 16, 107–116. https://doi.org/10.1046/j.1440-1703.2001.00376.x.
Jacobsen, A.L., Agenbag, L., Esler, K.J., Pratt, R.B., Ewers, F.W., Davis, S.D., 2007. Xylem density, biomechanics and anatomical traits correlate with water stress in 17 evergreen shrub species of the Mediterranean-type climate region of South Africa. J. Ecol. 95, 171–183. https://doi.org/10.1111/j.1365-2745.2006.01186.x.
Johnson, D.B., Moore, W.E., Zank, L.C., 1961. The spectrophotometric determination of lignin in small wood samples. Tappi J. 44, 793–798.
Kagawa, A., Naito, D., Sugimoto, A., Maximov, T.C., 2003. Effects of spatial and temporal variability in soil moisture on widths and $\delta^{13}C$ values of eastern Siberian tree rings. J. Geophys. Res. Atmos. 108, 61–68. https://doi.org/10.1029/2002JD003019.
Keeling, C.D., 1979. The Suess effect: 13Carbon-14Carbon interrelations. Environ. Int. 2, 229–300. https://doi.org/10.1016/0160-4120(79)90005-9.
Keppler, F., Kalin, R.M., Harper, D.B., McRoberts, W.C., Hamilton, John T.G., 2004. Carbon isotope anomaly in the major plant C1 pool and its global biogeochemical implications. Biogeosciences 1, 123–131. https://doi.org/10.5194/bgd-1-393-2004.
Keppler, F., Harper, D.B., Kalin, R.M., Meier-Augenstein, W., Farmer, N., Davis, S., Schmidt, H.L., Brown, D.M., 2007. Stable hydrogen isotope ratios of lignin methoxyl groups as a paleoclimate proxy and constraint of the geographical origin of wood. New Phytol. 176, 600–609. https://doi.org/10.1111/j.1469-8137.2007.02213.x.
Keppler, F., Hamilton, J.T.G. Tra, Keppler, F., Hamilton, J.T.G., 2008. Tracing the geographical origin of early potato tubers using stable hydrogen isotope ratios of methoxyl groups. Isot. Environ. Health Stud. 44, 337–347. https://doi.org/10.1080/10256010802507383.
Khaliq, M.N., Cunnane, C., 1996. Modelling point rainfall occurrences with the modified Bartlett-Lewis rectangular pulses model. J. Hydrol. 180, 109–138. https://doi.org/10.1016/0022-1694(95)02894-3.
Knorre, A.A., Siegwolf, R.T.W., Saurer, M., Sidorova, O.V., Vaganov, E.A., Kidvanov, A.V., 2010. Twentieth century trends in tree ring stable isotopes ($\delta^{13}C$ and $\delta^{18}O$) of *Larix sibirica* under dry condition in the forest steppe in Siberia. J. Geophys. Res. Atmos. 115 (G3). https://doi.org/10.1029/2009JG000930.
Koehler, L., Telewski, F., 2006. Biomechanics and transgenic wood. Am. J. Bot. 93, 1433–1438. https://doi.org/10.3732/ajb.93.10.1433.
Labuhn, I., Daux, V., Pierre, M., Stievenard, M., Girardclos, O., Féron, A., Genty, D., Masson-Delmotte, V., Mestre, O., 2014. Tree age, site and climate controls on tree ring cellulose $\delta^{18}O$: A case study on oak trees from south-western France. Dendrochronologia 32, 78–89. https://doi.org/10.1016/j.dendro.2013.11.001.
Lam, K.C., Ibrahim, R., Behdad, B., Dayanandan, S.D., 2007. Structure, function, and evolution of plant O-methyltransferases. Genome 50, 1001–1013. https://doi.org/10.1139/g07-077.
Lan, W., Rencoret, J., Lu, F., Karlen, S.D., Smith, B.G., Harris, P.J., Carlos del Rio, J., Ralph, J., 2016. Tricin-lignins: Occurrence and quantitation of tricin in relation to phylogeny. Plant J. 88, 1046–1057. https://doi.org/10.1111/tpj.13315.
Lapierre, C., Monties, B., Rolando, C., 1986. Thioacidolysis of poplar lignins: identification of monomeric syringyl products and characterization of guaiacyl-syringyl lignin fractions. Holzforschung 40, 113–118. https://doi.org/10.1515/hfsg.1986.40.2.113.
Leavitt, S., 2008. Tree-ring isotopic pooling without regard to mass: No difference from averaging $\delta^{13}C$ values of each tree. Chem. Geol. 252, 52–55. https://doi.org/10.1016/j.chemgeo.2008.01.014.
Leavitt, S., 2010. Tree-ring C-H–O isotope variability and sampling. Sci. Total Environ. 408, 5244–5253. https://doi.org/10.1016/j.scitotenv.2010.07.057.
Leavitt, S., Treydte, K., Liu, Y., 2010. Environment in time and space: opportunities from tree-ring isotope networks. In: West, J., Bowen, G., Dawson, T. (Eds.), Isoscapes: Understanding Movement, Pattern, and Process on Earth Through Isotope Mapping. Springer, Dordrecht, the Netherlands, pp. 113–135.
Lee, H.J., Feng, X.J., Mastalerz, M., Feakins, S.J., 2019. Characterizing lignin: combining lignin phenol, methoxy quantification, and dual stable carbon and hydrogen isotopic techniques. Org. Geochem. 136, 103894. https://doi.org/10.1016/j.orggeochem.2019.07.003.
Li, L.G., Popko, J.L., Zhang, X.H., Osakabe, K., Tasi, C.J., Joshi, C.P., Chiang, V.L., 1997. A novel multifunctional O-methyltransferase implicated in a dual methylation pathway associated with lignin biosynthesis in loblolly pine. PNAS 94, 5431–5466. https://doi.org/10.1073/pnas.94.10.5461.
Lim, K.J., Paasela, T., Harju, A., Venäläinen, M., Paulin, L., Auvinen, P., Kärkkäinen, K., Teeri, T.H., 2016. Developmental changes in Scots pine transcriptome during heartwood formation. Plant Physiol. 172, 1403–1417. https://doi.org/10.1104/pp.16.01082.
Lima, T.R.A., Carvalho, E.C.D., Martins, F.R., Oliveira, R.S., Miranda, R.S., Müller, C.S., Pereira, L., Bittencourt, P.R.L., Sobczak, J.C.M.S.M., Gomes-Filho, E., Costa, R.C., Araújo, F.S., 2018. Lignin composition is related to xylem embolism resistance and leaf life span in trees in a tropical semiarid climate. New Phytol. 219, 1252–1262. https://doi.org/10.1111/nph.15211.
Liu, X.H., An, W.L., Treydte, K., Wang, W.Z., Xu, G.B., Zeng, X.M., Wu, G.J., Wang, B., Zhang, X.W., 2015. Pooled versus separate tree-ring δD measurements, and implications for reconstruction of the Arctic Oscillation in northwestern China. Sci. Total Environ. 511, 584–594. https://doi.org/10.1016/j.scitotenv.2015.01.002.
Liu, X.H., Zhang, X.W., Zhao, L.J., Xu, G.B., Wang, L.X., Sun, W.Z., Zhang, Q.L., Wang, W.Z., Zeng, X.M., Wu, G.J., 2017. Tree ring $\delta^{18}O$ reveals no long-term change of atmospheric water demand since 1800 in the northern Great Hinggan Mountains. China. J. Geophys. Res. Atmos. 122, 6697–6712. https://doi.org/10.1002/2017JD026660.
Liu, X.H., Zhao, L.J., Voelker, S., Xu, G.B., Zeng, X.M., Zhang, X.W., Zhang, L.N., Sun, W.Z., Zhang, Q.L., Wu, G.J., Li, X.Q., 2019a. Warming and CO_2 enrichment modify the ecophysiological responses of *Larix gmelinii* and *Mongolia pine* during the past century in the permafrost of northeastern China. Tree Physiol. 39, 88–103. https://doi.org/10.1093/treephys/tpy060.
Liu, Y., Bao, G., Song, H., Cai, Q.F., Sun, J.Y., 2009. Precipitation reconstruction from Hailar pine (*Pinus sylvestris* var. *mongolica*) tree rings in the Hailar region, Inner Mongolia, China back to 1865 CE. Palaeogeogr. Palaeocl. Palaeoecol. 282, 81–87. https://doi.org/10.1016/j.palaeo.2009.08.012.
Liu, Y., Wang, R.Y., Leavitt, S.W., Song, H.M., Linderholm, H.W., Li, Q., An, Z.S., 2012. Individual and pooled tree-ring stable-carbon isotope series in Chinese pine from the Nan Wutai region, China: common signal and climate relationships. Chem. Geol. 330–331, 17–26. https://doi.org/10.1016/j.chemgeo.2012.08.008.
Liu, Y., Song, H.M., Sun, C.F., Song, Y., Cai, Q.F., Liu, R.S., Lei, Y., Li, Q., 2019b. The 600-mm precipitation isoline distinguishes tree-ring-width responses to climate in China. Natl. Sci. Rev. 6, 183–192. https://doi.org/10.1093/nsr/nwy101.
Loader, N.J., Robertson, I., Barker, A.C., Switsur, V.R., Waterhouse, J.S., 1997. An improved technique for the batch processing of small whole wood samples to α-cellulose. Chem. Geol. 136, 313–317. https://doi.org/10.1016/S0009-2541(96)00133-7.
Martone, P.T., Estevez, J.M., Lu, F.C., Ruel, K., Denny, M.W., Somerville, C., Ralph, J., 2009. Discovery of lignin in seaweed reveals convergent evolution of cell-wall architecture. Curr. Biol. 19, 169–175. https://doi.org/10.1016/j.cub.2008.12.031.
Maury, S., Delaunay, A., Mesnard, F., Crônier, D., Chabbert, B., Geoffroy, P., Legrand, M., 2010. O-methyltransferase(s)-suppressed plants produce lower amounts of phenolic vir inducers and are less susceptible to *Agrobacterium tumefaciens* infection. Planta 232, 975–986. https://doi.org/10.1007/s00425-010-1230-x.
McCarroll, D., Loader, N.J., 2004. Stable isotopes in tree rings. Quat. Sci. Rev. 23, 771–801. https://doi.org/10.1016/j.quascirev.2003.06.017.
Meier-Augenstein, W., 2019. From stable isotope ecology to forensic isotope ecology – Isotopes' tales. Forensic Sci. Int. 300, 89–98. https://doi.org/10.1016/j.forsciint.2019.04.023.
Meier-Augenstein, W., Schimmelmann, A., 2019. A guide for proper utilisation of stable isotope reference materials. Isot. Environ. Health Stud. 55, 113–128. https://doi.org/10.1080/10256016.2018.1538137.
Millers, M., 2013. The proportion of heartwood in conifer (*Pinus sylvestris* L., *Picea abies* [L.] H. Karst.) trunks and its influence on trunk wood moisture. J. For. Sci. 59, 295–300. https://doi.org/10.17221/29/2013-JFS.
Mischel, M., Esper, J., Keppler, F., Greule, M., Werner, W., 2015. $\delta^{2}H$, $\delta^{13}C$ and $\delta^{18}O$ from whole wood, α-cellulose and lignin methoxyl groups in *Pinus sylvestris*: a multi-parameter approach. Isotopes Environ. Health Studies 51, 1–16. https://doi.org/10.1080/10256016.2015.1056181.
Nakada, R., Fukatsu, E., 2012. Seasonal variation of heartwood formation in *Larix kaempferi*. Tree Physiol. 32, 1497–1508. https://doi.org/10.1093/treephys/tps108.
Nakashima, J., Chen, F., Jackson, L., Shadle, G., Dixon, R.A., 2008. Multi-site genetic modification of monolignol biosynthesis in alfalfa (*Medicago sativa*): effects on lignin composition in specific cell types. New Phytol. 179, 738–750. https://doi.org/10.1111/j.1469-8137.2008.02502.x.
Pereira, L., Domingues-Junior, A.P., Jansen, S., Choat, B., Mazzafera, P., 2017. Is embolism resistance in plant xylem associated with quantity and characteristics of lignin? Trees 32, 349–358. https://doi.org/10.1007/s00468-017-1574-y.
Pilate, G., Déjardin, A., Leplé, J., 2012. Chapter 1 – Field trials with lignin-modified transgenic trees. Adv. Bot. Res. 61, 1–36. https://doi.org/10.1016/B978-0-12-416023-1.00001-X.
Piqueras, S., Füchtner, S., de Oliveira, R.R., Gómez-Sánchez, A., Jelavić, S., Keplinger, T., de Juan, A., Thygesen, L.G., 2020. Understanding the formation of heartwood in larch using synchrotron infrared imaging combined with multivariate analysis and atomic force microscope infrared spectroscopy. Front. Plant Sci. 10, 1–15. https://doi.org/10.3389/fpls.2019.01701.
Riechelmann, D.F.C., Greule, M., Treydte, K., Esper, J., Keppler, F., 2016. Climate signals in $\delta^{13}C$ of wood lignin methoxyl groups from high-elevation larch trees. Palaeogeogr. Palaeocl. Palaeoecol. 445, 60–71. https://doi.org/10.1016/j.palaeo.2016.01.001.
Riechelmann, D.F.C., Greule, M., Siegwolf, R.T.W., Anhäuser, T., Esper, J., Keppler, F., 2017. Warm season precipitation signal in $\delta^{2}H$ values of wood lignin methoxyl groups from high elevation larch trees in Switzerland. Rapid Commun. Mass Spec. 31, 1589–1598. https://doi.org/10.1002/rcm.7938.
Robertson, I., Loader, N.J., McCarroll, D., Carter, A.H.C., Cheng, L., Leavitt, S.W., 2004.

^{13}C of tree-ring lignin as an indirect measure of climate change. Water Air Soil Poll. 4, 531–544. https://doi.org/10.1023/B:WAFO.0000028376.06179.af.
Robinson, A.R., Mansfield, S.D., 2009. Rapid analysis of poplar lignin monomer composition by a streamlined thioacidolysis procedure and near-infrared reflectance-based prediction modeling. Plant J. 58, 706–714. https://doi.org/10.1111/j.1365-313X.2009.03808.x.
Roden, J.S., Lin, G.H., Ehleringer, J.R., 2000. A mechanistic model for interpretation of hydrogen and oxygen isotope ratios in tree-ring cellulose. Geochim. Cosmochim. Acta 64, 21–35. https://doi.org/10.1016/S0016-7037(99)00195-7.
Saito, K., Watanabe, Y., Shirakawa, M., Matsushita, Y., Imai, T., Koike, T., Sano, Y., Funada, R., Fukazawa, K., Fukushima, K., 2012. Direct mapping of morphological distribution of syringyl and guaiacyl lignin in the xylem of maple by time of flight secondary ion mass spectrometry. Plant J. 69, 542–552. https://doi.org/10.1111/j.1365-313X.2011.04811.x.
Schweingruber, F.H., Briffa, K.R., Nogler, P., 1993. A tree-ring densitometric transect from Alaska to Labrador. Internat. J. Biometeorol. 37, 151–169. https://doi.org/10.1007/BF01212625.
Sessions, A.L., 2016. Factors controlling the deuterium contents of sedimentary hydrocarbons. Org. Geochem. 96, 43–64. https://doi.org/10.1016/j.orggeochem.2016.02.012.
Silva Moura, J.C.M., Bonine, C.A.V., Viana, J.D.F., Dornelas, M.C., Mazzafera, P., 2010. Abiotic and biotic stresses and changes in the lignin content and composition in plants. J. Integr. Plant Biol. 52, 360–376. https://doi.org/10.1111/j.1744-7909.2010.00892.x.
Somerville, C., Bauer, S., Brininstool, G., Facette, M., Hamann, T., Milen, J., Osborne, E., Paredez, A., Persson, S., Paab, T., Vorwerk, S., Youngs, H., 2004. Toward a systems approach to understanding plant cell walls. Science 306, 2206–2211. https://doi.org/10.1126/science.1102765.
Song, K.L., Liu, B., Jiang, X.M., Yin, Y.F., 2011. Cellular changes of tracheids and ray parenchyma cells from cambium to heartwood in *Cunninghamia lanceolata*. J. Trop. For. Sci. 23, 478–487. https://doi.org/10.1139/X11-123.
Stackpole, D.J., Vaillancourt, R.E., Alves, A., Rodrigues, J., Potts, B.M., 2011. Genetic variation in the chemical components of *Eucalyptus globulus* wood. G3 Genes Genom. Genet. 1, 151–159. https://doi.org/10.1534/g3.111.000372.
Sternberg, L.D.L., 1988. D/H ratios of environmental water recorded by D/H ratios of plant lipids. Nature 333, 59–61. https://doi.org/10.1038/333059a0.
Suárez, M., Thorne, B., 2009. Rate, amount, and distribution pattern of alimentary fluid transfer via trophallaxis in three species of termites (Isoptera: Rhinotermitidae, Termopsidae). Ann. Entomol. Soc. Am. 93, 145–155. https://doi.org/10.1603/0013-8746(2000)093[0145:RAADPO]2.0.CO;2.
Szymczak, S., Joachimski, M.M., Bräuning, A., Hetzer, T., Kuhlemann, A., 2012. Are pooled tree ring δ^{13}C and δ^{18}O series reliable climate archives? A case study of *Pinus nigra* spp. *laricio* (Corsica/France). Chem. Geol. 308–309, 40–49. https://doi.org/10.1016/j.chemgeo.2012.03.013.
Tang, K.L., Feng, X.H., Ettl, G.J., 2000. The variations in δD of tree rings and the implications for climatic reconstruction. Geochim. Cosmochim. Acta 64, 1663–1673. https://doi.org/10.1016/S0016-7037(00)00348-3.
Tardif, J.C., Conciatori, F., Leavitt, S.W., 2008. Tree rings, δ^{13}C and climate in *Picea glauca* growing near Churchill, subarctic Manitoba Canada. Chem. Geol. 252, 88–101. https://doi.org/10.1016/j.chemgeo.2008.01.015.
Tian, Q.H., Gou, X.H., Zhang, Y., Peng, J.F., Wang, J.S., Chen, T., 2007. Tree-ring based drought reconstruction (A.D. 1855–2001) for the Qilian Mountains Northwestern China. Tree-Ring Res. 63, 27–36. https://doi.org/10.3959/1536-1098-63.1.27.
Treydte, K., Schleser, G.H., Schweingruber, F.H., Winiger, M., 2001. The climatic significance of δ^{13}C in subalpine spruces (Lötschental, Swiss Alps): A case study with respect to altitude, exposure and soil moisture. Tellus 53, 593–611. https://doi.org/10.3402/tellusb.v53i5.16639.
Treydte, K., Schleser, G.H., Helle, G., Frank, D.C., Winiger, M., Haug, G.H., Esper, J., 2006. The twentieth century was the wettest period in northern Pakistan over the past millennium. Nature 440, 1179–1182. https://doi.org/10.1038/nature04743.
Vanholme, R., Demedts, B., Morreel, K., Ralph, J., Boerjan, W., 2010. Lignin biosynthesis and structure. Plant Physiol. 153, 895–905. https://doi.org/10.1104/pp.110.155119.
Vanholme, R., Meester, B.D., Ralph, J., Boerjan, W., 2019. Lignin biosynthesis and its integration into metabolism. Curr. Opin. Biotech. 59, 230–239. https://doi.org/10.1016/j.copbio.2019.02.018.
Verheyden, A., Roggeman, M., Bouillon, S., Elskens, M., Beeckman, H., Koedam, N., 2005. Comparison between δ^{13}C of α-cellulose and bulk wood in the mangrove tree *Rhizophora mucronata*: implications for dendrochemistry. Chem. Geol. 219, 275–282. https://doi.org/10.1016/j.chemgeo.2005.02.015.
Voelker, S.L., Lachenbruch, B., Meinzer, F.C., Kitin, P., Strauss, S.H., 2011. Transgenic poplars with reduced lignin show impaired xylem conductivity, growth efficiency and survival. Plant Cell Environ. 34, 655–668. https://doi.org/10.1111/j.1365-3040.2010.02270.x.
Wang, Y.B., Liu, X.H., Anhäuser, T., Lu, Q.Q., Zeng, X.M., Zhang, Q.L., Wang, K.Y., Zhang, L.N., Zhang, Y., Keppler, F., 2020. Temperature signal recorded in δ^{2}H and δ^{13}C values of wood lignin methoxyl groups from a permafrost forest in northeastern China. Sci. Total Environ. 727, 138558. https://doi.org/10.1016/j.scitotenv.2020.138558.
Werner, R.A., Brand, W.A., 2001. Referencing strategies and techniques in stable isotope ratio analysis. Rapid Commun. Mass Spectrom. 15, 501–519. https://doi.org/10.1002/rcm.258.
Xia, Y., Liu, J., Wang, Y., Zhang, X.X., Shen, Z.G., Hu, Z.B., 2018. Ectopic expression of *Vicia sativa* Caffeoyl-CoA O-methyltransferase(*VsCCoAOMT*) increases the uptake and tolerance of cadmium in Arabidopsis. Environ. Exp. Bot. 145, 47–53. https://doi.org/10.1016/j.envexpbot.2017.10.019.
Zabala, G., Zou, J.J., Tuteja, J., Gonzalez, D.O., Clough, S.J., Vodkin, L.O., 2006. Transcriptome changes in the phenylpropanoid pathway of *Glycine max* in response to *Pseudomonas syringae* infection. BMC Plant Biol. 6, 26–44. https://doi.org/10.1186/1471-2229-6-26.
Zeisel, S., 1885. Über ein Verfahren zum quantitativen Nachweise von Methoxyl. Monatsh. Chem. 6, 989–997.
Zeng, X.M., Liu, X.H., Treydte, K., Evans, M.N., Wang, W.Z., An, W.L., Sun, W.Z., Xu, G.B., Wu, G.J., Zhang, X.W., 2017. Climate signals in tree-ring δ^{18}O and δ^{13}C from southeastern Tibet: Insights from observations and forward modelling of intra to interdecadal variability. New Phytol. 216, 1104–1118. https://doi.org/10.1016/j.epsl.2016.03.011.
Zhang, T.W., Yuan, Y.J., Wei, W.S., Yu, S.L., Zhang, R.B., Chen, F., Shang, H.M., Qin, L., 2014. A tree-ring based precipitation reconstruction for the Mohe region in the northern Greater Higgnan Mountains, China, since 1724 CE. Quat. Res. 82, 14–21. https://doi.org/10.1016/j.yqres.2014.01.007.
Zhang, X.W., Liu, X.H., Zhang, Q.L., Zeng, X.M., Xu, G.B., Wu, G.J., Wang, W.Z., 2018. Species-specific tree growth and intrinsic water-use efficiency of *Larix gmelinii (Larix gmelinii*) and *Mongolian pine (Pinus sylvestris* var. *mongolica*) growing in a boreal permafrost region of the Greater Hinggan Mountains. Northeastern China. Agric. For. Meteorol. 248, 145–155. https://doi.org/10.1016/j.agrformet.2017.09.013.
Zobel, B.J., van Buijtenen, J.P., 1989. Wood Variation: Its Causes and Control. Springer-Verlag, Berlin, pp. 7–421.